

# LONGITUDINAL RESONANCES AND EMITTANCE GROWTH USING QWR/HWR IN A LINAC

P. Bertrand, GANIL, Caen, France

## Abstract

In the frame of the SPIRAL 2 project at GANIL [1], we present an analytical approach allowing us to understand in a simple way the longitudinal behaviour of the beam, transmitted in a LINAC designed with QWR or HWR cavities. In particular, we make appear the strong relationship with the Henon map properties.

## INTRODUCTION

The best and ultimate way to check the end-to-end beam behaviour through a given designed LINAC, and perform alignment studies, is certainly to track a huge number of particles through 3D realistic electromagnetic fields. (see [2] in the case of SPIRAL 2).

However, it is useful to dispose of simplified analytical models in order to understand better the origin of anomalies and possible emittance growths. In what follows, we focus on the longitudinal behaviour of the beam when getting through QWR/HWR cavities.

## ANALYTICAL FORMULAE

It is possible to approach very well the potential and electric fields of QWR/HWR cavities with the following analytical relations:

$$\begin{aligned}
 V &= \frac{9}{16} V_{stem} (\cos(kz) - \frac{1}{9} \cos(3kz) + \frac{8}{9}) \sin(\omega t + \varphi) \\
 E_z &= \frac{9}{16} k V_{stem} (\sin(kz) - \frac{1}{3} \sin(3kz)) \sin(\omega t + \varphi) \\
 E_r &= -r \frac{9}{32} k^2 V_{stem} (\cos(kz) - \cos(3kz)) \sin(\omega t + \varphi) \\
 \omega &= 2\pi f_{hf} \quad ; \quad k = \frac{2\pi}{\beta_0 \lambda} \quad ; \quad \lambda = \frac{c}{f_{hf}}
 \end{aligned} \tag{1}$$

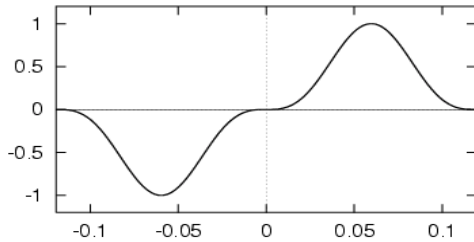


Figure 1: Longitudinal  $E_z(z)$  component defined by the relation (1), for  $f_{hf} = 88$  Mhz and  $\beta_0=0.07$ .

## LONGITUDINAL FOCUSING

By integrating the motion along the accelerating z-axis, we obtain the energy gain and deduce an analytical and realistic expression of the transit time factor  $T(s)$  :

$$s = \frac{\beta}{\beta_0} \quad ; \quad T(s) = \frac{16 \sin(\pi/s) s^4}{\pi(1-s^2)(1-9s^2)} \tag{2}$$

$$\Delta W = \frac{9\pi}{16} q V_{stem} T(s) \cos(\varphi) \tag{3}$$

We can notice that  $T(s)$  is equal to 1 for  $\beta=\beta_0$ , but that it does not correspond exactly to the optimum of the curve, which is achieved for  $\beta_0^*=1.1\beta_0$  with  $T(\beta_0^*/\beta_0)=1.0115$ .

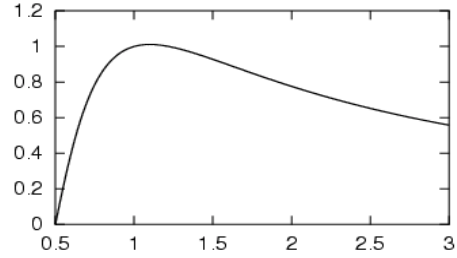


Figure 2: Analytical Transit Time Factor  $T(s)$  given by (2)

In terms of relative impulsions, the equation (3) becomes :

$$\frac{\Delta p}{p} = \alpha \cos(\varphi) \quad ; \quad \alpha = \frac{9\pi}{16} \frac{q V_{stem}}{m_0 c^2} \frac{T(s)}{\gamma \beta_0 s^2}$$

which gives between the central particle with the phase  $\varphi$  and another one with the phase  $\varphi+\delta\varphi$  :

$$\begin{aligned}
 \delta\varphi &= \frac{2\pi}{\beta\lambda} \delta z \\
 \frac{\delta p}{p} &\approx -\alpha (\sin(\varphi) \delta\varphi + \cos(\varphi) \frac{\delta\varphi^2}{2}) \\
 &= -\alpha \frac{2\pi}{\beta\lambda} \sin(\varphi) \left( \delta z + \frac{1}{2} \frac{\cos(\varphi)}{\sin(\varphi)} \frac{2\pi}{\beta\lambda} \delta z^2 \right)
 \end{aligned} \tag{4}$$

This corresponds to the focusing longitudinal linear term of the cavity, and an *additional second order contribution*, the effect of which we will study in what follows.

## RECURRENCES

In order to simplify the above expressions, we introduce the following notations :

$$\frac{1}{f} = \alpha \frac{2\pi}{\beta\lambda} \sin(\varphi) ; \quad a = \frac{\cos(\varphi)}{\sin(\varphi)} \frac{2\pi}{\beta\lambda} ; \quad g = \frac{a}{2f} \quad (5)$$

$$u = \delta z \quad ; \quad v = \frac{\delta p}{p} \quad (6)$$

Lets' consider one cell composed of a drift of length  $L$ , one cavity, and another drift of length  $L$ , and let's calculate the evolution of  $(u,v)$  :

$$u_1 = u_0 + 2Lv_0 - (L/f)(u_0 + Lv_0) - gL(u_0 + Lv_0)^2 \quad (7)$$

$$v_1 = v_0 - (1/f)(u_0 + Lv_0) - g(u_0 + Lv_0)^2$$

We introduce the dimensionless variables  $(x,y)$  and the phase advance per focusing period  $\mu$  :

$$x = a(u + Lv)$$

$$y = a(u - Lv)$$

$$\cos(\mu) = 1 - L/f$$

which gives a transformation depending only upon  $\mu$  :

$$x_1 = -y_0 + 2 \cos(\mu)x_0 - (1 - \cos(\mu))x_0^2 \quad (8)$$

$$y_1 = x_0$$

Of course, the tuning of a LINAC does not correspond to a constant phase advance along the machine, and we have neglected the increase of the energy through the cavity .

However, the academic study of the recurrence  $(u_n, v_n)$  in (7) or  $(x_n, y_n)$  in (8) around the fixed point  $(0,0)$  for a constant  $\mu$  is very instructive: with a small program and given values of  $(\mu, \varphi, \beta_0, L)$ , we can generate a huge set of initial points  $(\delta\varphi, \delta p/p)$ . Then, by applying a big number of recurrences, we find out the stable area. The following figures correspond to  $(\varphi, \beta_0, L) = (30^\circ, 0.07, 0.5\text{m})$ .

The figure (3) shows how the particles disappear, and how the dynamic aperture is created in the case  $\mu=92^\circ$ , making appear a very small central stable area around the fixed point and peripheral tiny islets.

The figure (4) shows that for  $\mu > 90^\circ$ , the stable area is greatly reduced. The figure (5) gives the deformation of a bunch initially matched for each chosen phase advance, and going through 2 successive cells : all this confirms that even without space charge, a LINAC must be designed and tuned in order to work below  $90^\circ$  and to limit the emittance growth.

The figure (6) gives us the dynamic aperture obtained as a function of  $\mu$ , making appear clearly the resonances appearing near  $90^\circ$  and  $120^\circ$ , as already mentioned in [4] in the case of transverse dynamics with sextupole effects.

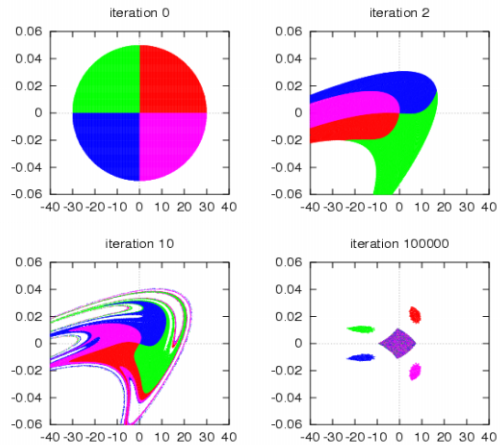


Figure 3 :  $(\delta\varphi, \delta p/p)$  portrait evolution and final acceptance for  $\mu=92^\circ$ .

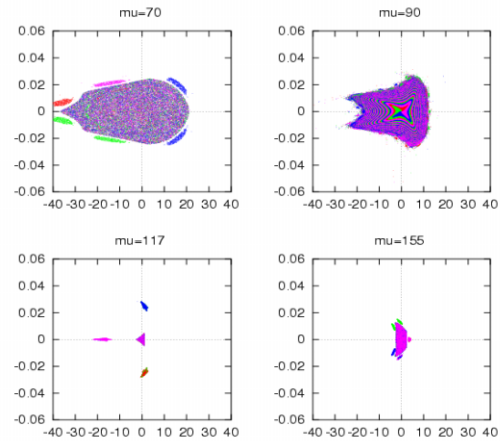


Figure 4 :  $(\delta\varphi, \delta p/p)$  stable areas for phase advances per period equal to  $70^\circ, 90^\circ, 117^\circ$  and  $155^\circ$ .

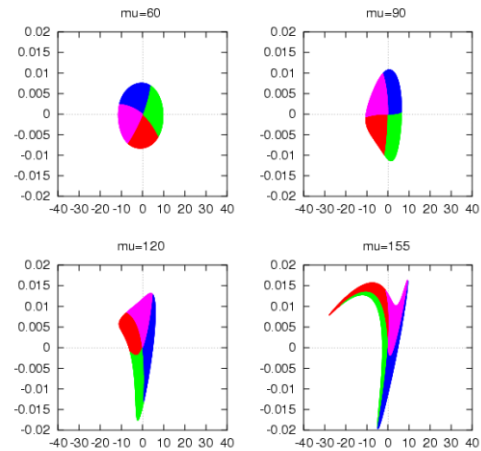


Figure 5 :  $(\delta\varphi, \delta p/p)$  portraits after two cells for a geometrical emittance  $57\pi \text{ mm.mrad}$ , and the phase advance values :  $\mu = 60^\circ, 90^\circ, 120^\circ$  and  $155^\circ$ .

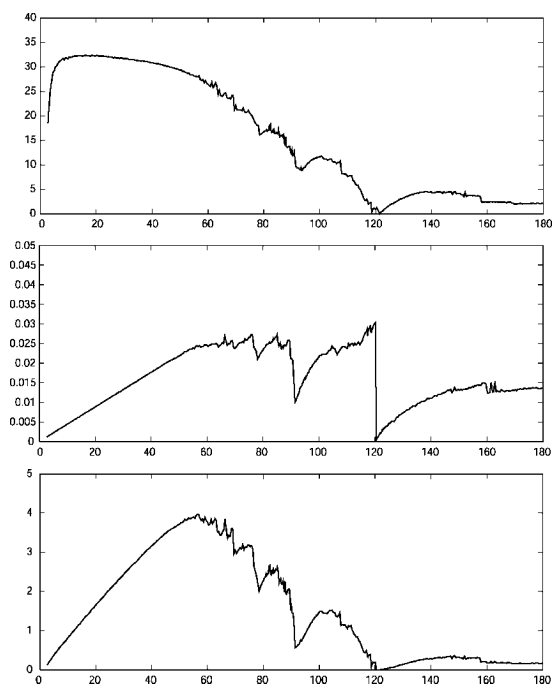


Figure 6 : phase, impulsion and acceptance as a fonction of the phase advance per focusing period.

## RELATION WITH THE HENON MAP

Lets's now reconsider the recurrence given by (8) :

$$\begin{aligned} x_{n+1} &= -y_n + 2 \cos(\mu)x_n - (1 - \cos(\mu))x_n^2 & (9) \\ y_{n+1} &= x_n \end{aligned}$$

and the Henon recurrence :

$$\begin{aligned} X_{n+1} &= Y_n + 1 - \tilde{\alpha}X_n^2 & (10) \\ Y_{n+1} &= \tilde{\beta}X_n \\ (-1, -1) &\leq (\tilde{\alpha}, \tilde{\beta}) \leq (4, 1) \end{aligned}$$

Except for the particular case  $\mu=90^\circ$ , the two recurrences are equivalent provided that :

$$\begin{aligned} X &= A + Bx \\ \tilde{\beta} &= -1 \\ \tilde{\alpha} &= -\cos(\mu)(2 - \cos(\mu)) \\ A &= \frac{1}{2 - \cos(\mu)} \\ B &= -\frac{1 - \cos(\mu)}{\cos(\mu)(2 - \cos(\mu))} \end{aligned}$$

We notice that the value  $\mu = 120^\circ$  corresponds to  $\tilde{\alpha} = 5/4$  with a Henon stable region reduced to the fixed point  $(2/5, -2/5)$ . It corresponds to the nul second derivative of the function  $\tilde{\alpha}(\mu)$ .

If we take into account the increase of energy through the cavity we obtain :

$$\begin{aligned} e &= \frac{p_{in}}{p_{out}} = -\tilde{\beta} \leq 1 \\ X &= \frac{2}{1+e}(A + Bx) \\ \tilde{\alpha} &= -\left(\frac{1+e}{2}\right)^2 \cos(\mu)(2 - \cos(\mu)) \end{aligned}$$

Following the Renormalization Group Reduction method mentionned in [5], we can introduce a formal parameter  $\epsilon$  in the nonlinear term of [8]. Then we make appear analytically and successively the resonances  $120^\circ$ ,  $90^\circ$ ,  $72^\circ$  etc....

## CONCLUSION

The use of simplified nonlinear recurrences in the longitudinal phase plane allows us to make clearly appear the resonances for phase advances equal to  $90^\circ$  and  $120^\circ$  (and also others which are less dangerous). Moreover the Henon map approach and the RG method, with one or several cavities per cell, and generalized to variable coefficients, could give a useful tool to understand better the longitudinal beam behaviour in a LINAC.

## ACKNOWLEDGEMENT

We would like to thank the student Benjamin Roure for his working with passion on the subject treated.

## REFERENCES

- [1] M.H. Moscatello and the SPIRAL 2 project group. SPIRAL 2 at GANIL . LINAC 2004. Lubeck.
- [2] R. Duperrier and al. Status Report on the Beam Dynamics Developments for the SPIRAL 2 Project, EPAC 2004.
- [3] G. Franchetti, G. Turchetti. A Henon map approach to the transverse dynamics of off momentum particles . AIP, New York. (1999)
- [4] L. Nadolski. Application de l'Analyse en Fréquence à l'Etude de la Dynamique des Sources de Lumière. Université Paris XI . Thesis. (2001).
- [5] S.I. Tzenov, R.C. Davidson, Renormalisation group reduction of the Henon map and application to the transverse betatron motion in cyclic accelerators. New Journal of Physics. (2003)